

strong action of ultrasound is due to the dependence of viscosity on density or to second-order viscosity, both of which are totally unknown for any liquid crystal. Another possibility to generate vortices, but no straight flow, is Bénard's instability in a thermal gradient.¹² The experimental reports^{6,7} do not refer to this mechanism which would probably have been easy to recognize (for instance, by very long response times).

In summary, it seems that the proposed mechanism of sound action on nematics is plausible and may provide a means to explore novel material properties. Our high estimate of the threshold is based on fairly unfavorable assumptions. The use of larger viscosities and thicknesses than those inserted above would lower the preliminary theoretical value by orders of magnitude.¹³

¹L. D. Landau and E. M. Lifshitz, *Fluid Mechanics* (Pergamon, Oxford, 1966).

²P. M. Morse and K. U. Ingard, *Theoretical Acoustics* (McGraw-Hill, New York, 1968).

³The oscillatory motion of the nematic director affects the coefficients in (2) and (3), but need not be considered explicitly. Besides the two "translational" modes in the x, z plane, there is an "orientational"

mode involving curvature elasticity but not density. It is damped within an extremely short distance and thus negligible. [See, e.g., P. Martinoty and S. Candau, *Mol. Cryst. Liquid Cryst.* **14**, 243 (1971).]

⁴D. Forster, T. C. Lubensky, P. C. Martin, J. Swift, and P. S. Pershan, *Phys. Rev. Lett.* **26**, 1016 (1971).

⁵R. Williams, *J. Chem. Phys.* **39**, 384 (1963).

⁶H. Mailer, K. L. Litkins, T. R. Taylor, and J. L. Ferguson, *Appl. Phys. Lett.* **18**, 105 (1971). Their observed sound-induced birefringence of a normally aligned layer suggests $c < 0$ and thus $\alpha > 0$. This appears reasonable, the viscosity and probably also the viscoelasticity being largest along the nematic axis [see K. A. Kemp and S. V. Letcher, *Phys. Rev. Lett.* **27**, 1634 (1971); M. E. Mullen, B. Lüthi, and M. J. Stephen, *Phys. Rev. Lett.* **28**, 799 (1972)].

⁷L. W. Kessler and S. P. Sawyer, *Appl. Phys. Lett.* **17**, 440 (1970).

⁸C. Gähwiller, *Phys. Lett.* **36A**, 311 (1971).

⁹Kemp and Letcher, Ref. 6.

¹⁰Mullen, Lüthi, and Stephen, Ref. 6.

¹¹A shear viscosity of 10 P has been observed at room temperature with a nematic liquid crystal by C. Gähwiller (to be published).

¹²E. Guyon and P. Pieranski, *C. R. Acad. Sci., Paris* **274B**, 656 (1972).

¹³The possible increase in sensitivity is limited by the requirement that the sample thickness be smaller than the sound absorption length. The absorption length in MBBA at 10 MHz should be roughly 1 cm, as may be deduced from the data of G. G. Natale and D. E. Commins, *Phys. Rev. Lett.* **28**, 1439 (1972).

Multiple Soliton Production and the Korteweg-de Vries Equation*

Noah Hershkowitz, Thomas Romesser, and David Montgomery

Department of Physics and Astronomy, University of Iowa, Iowa City, Iowa 52240

(Received 26 October 1972)

Compressive square-wave pulses are launched in a double-plasma device. Their evolution is interpreted according to the Korteweg-de Vries description of Washimi and Taniuti. Square-wave pulses are an excitation for which an explicit solution of the Schrödinger equation permits an analytical prediction of the number and amplitude of emergent solitons. Bursts of energetic particles (pseudowaves) appear above excitation voltages greater than an electron thermal energy, and may be mistaken for solitons.

A mathematical description of slightly nonlinear, one-dimensional, ion acoustic waves in a collisionless plasma with cold ions has been given by Washimi and Taniuti.¹ The resulting equation for the fractional perturbation of the ambient ion number density is the Korteweg-de Vries equation,^{2,3}

$$\frac{\partial}{\partial t} \frac{\delta n}{n_0} + \frac{\delta n}{n_0} \frac{\partial}{\partial x} \frac{\delta n}{n_0} + \frac{1}{2} \frac{\partial^3}{\partial x^3} \frac{\delta n}{n_0} = 0, \quad (1)$$

where $\delta n = \delta n(x, t)$ is the perturbation on the ion

number density, and n_0 is the steady-state constant density of the plasma. x is the spatial coordinate measured in units of the electron Debye length λ_D and t is the time measured in units of the inverse ion plasma frequency, ω_{pi}^{-1} . Equation (1) is written in a coordinate frame moving to the right with an ion acoustic speed $c_s = \lambda_D \omega_{pi}$.

Equation (1) has been intensively studied in the last decade.⁴⁻¹⁰ In particular, an asymptotic long-time solution has been given¹¹ which applies to density perturbations $\delta n(x, 0)/n_0$ which are pos-

itive (compressive) and of finite spatial extent. We shall be concerned in this article with the case where $\delta n(x, 0)/n_0$ is a finite square wave of magnitude $\delta n_0/n_0$.

The prediction for the long-time right-traveling part of the solution is a superposition of spatially separated "solitons" of the form [we now express the results in laboratory (cgs) units, but again in a coordinate frame which travels to the right with the ion acoustic speed c_s]

$$\delta n(x, t)/n_0 = \sum_j 2\epsilon_j \operatorname{sech}^2 \eta_j, \tag{2}$$

where $\epsilon_j = (\delta n_0/n_0)g_j$ and $g_j = |E_j|/V_0$. $E_j < 0$ is the j th negative eigenvalue of the Schrödinger equation

$$\partial^2 \psi / \partial \xi^2 + [E - V(\xi)] \psi = 0, \tag{3}$$

where $\xi = (2)^{1/3}x/\lambda_D$, with x measured in centimeters. $V(\xi)$ is an attractive square-well potential of depth $V_0 = [(2)^{1/3}/6]\delta n_0/n_0$, and of width $a(2)^{+1/3}$, with a the width of the laboratory pulse in units of λ_D ;

$$\eta_j = (\epsilon_j/3)^{1/2}(x - \frac{2}{3}\epsilon_j c_s t)/\lambda_D + \varphi_j,$$

where $c_s = (kT_e/m_i)^{1/2}$ and $\lambda_D = (kT_e/4\pi n_0 e^2)^{1/2}$. T_e is the electron temperature, m_i is the ion mass, and e is the electronic charge. $\varphi_j = -\frac{1}{2} \ln [c_j^2(0)/2|E_j|^{1/2}]$, where $c_j(0)$ is the coefficient of the $\exp[-|E_j|^{1/2}\xi]$ term in the $\xi \rightarrow \infty$ form of the normalized asymptotic eigenfunction to Eq. (3). $c_j(0)$ can be readily evaluated at the edge of the well at $t=0$.

Since the Schrödinger well is of finite depth, there will only be a finite number of bound states, and the sum in Eq. (2) will consist of a finite number of terms, one for each "soliton." The solitons will be arranged with those of largest amplitude traveling to the right, and all traveling with a speed $\frac{1}{3}(\delta n_{\max}/n_0)c_s$, $\frac{1}{3}$ of their maximum fractional density modulation times the ion acoustic speed c_s . Their spatial widths are inversely proportional to the square root of this fractional density modulation, and their temporal widths to its inverse $\frac{3}{2}$ power.

In addition to the right-traveling integral number of solitons, the solution also predicts a left-traveling, dispersing wave train.^{11,3}

We report here the results of an experimental test of these predictions for a square-wave pulse launched in a laboratory plasma. Experiments were carried out in the University of Iowa double-plasma (DP) device. The device is of the same type as that developed by Taylor, Baker, and Ikezi¹² to study the evolution of ion acoustic shocks.

Ikezi, Taylor, and Baker¹³ used the same kind of device to observe the propagation and interaction of single solitons, while Stern and Decker¹⁴ have used a DP device to generate ion-acoustic turbulent pulses. (See also Wong and Means.¹⁵)

Two argon plasmas are maintained in chambers (length 37 cm, diam 38 cm) separated by a negatively biased screen. Typical operating parameters were $T_e = 0.8$ to 1.5 eV, $T_i \approx 0.2$ eV, $n_0 \approx 10^8$ to 10^9 cm⁻³, and pressure $\approx 2 \times 10^{-4}$ Torr. The plasmas were adjusted so that there was less than 0.2 V difference in potential between the two chambers, so that no ion beam was present.¹⁵ It has been shown that the application of voltage pulses to one chamber (the "driver") relative to the other chamber (the "target") can efficiently launch compressive or rarefactive density pulses in the plasma.¹² The pulses may be studied with either a positively biased Langmuir probe or an electrostatic energy analyzer.¹⁶ More complete descriptions of the apparatus and these experiments will be reported elsewhere.

Three types of propagating phenomena are observed when compressive square pulses are applied to the driver plasma. Figure 1 shows the signals detected by a positively biased Langmuir probe located 20 cm from the screen. With low-amplitude ($\ll kT_e$) pulses, we detect essentially square pulses with propagation velocities equal to c_s (Fig. 1, curve *a*). As the applied pulse amplitude is increased (with fixed pulse width), the pulse velocity increases, and the leading edge (in time) sharpens into at least one narrow pulse (Fig. 1, curve *b*) which can be identified as a sol-

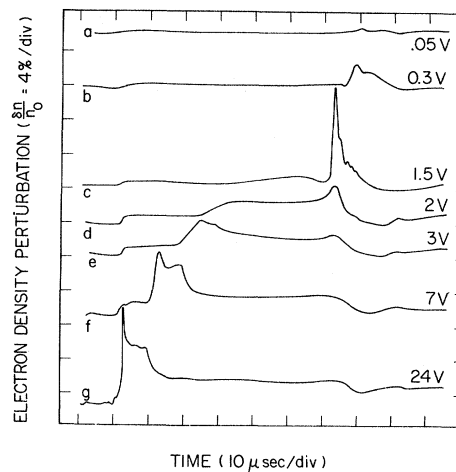


FIG. 1. Electron density versus time, 20 cm from the screen, following the application of 10- μ sec square pulses to the driver chamber. Signals are labeled by the square-pulse amplitude.

iton. The soliton (or solitons) increase in amplitude and speed with increasing applied voltage, reaching a maximum when the applied voltage is approximately equal to the electron temperature in eV (Fig. 1, curve *c*). Larger applied pulse voltages result in *reduction* in amplitude, broadening and slowing the soliton, and the emergence of new pulses ("pseudowaves"¹⁶⁻¹⁸).

The new pulses have velocities greater than the soliton velocities (Fig. 1, curve *d*). With increasing applied signal, the leading edges of the pseudowaves sharpen into pulses that are superficially similar in appearance to the solitons (Fig. 1, curves *e-g*). The solitons have continued to decrease in amplitude and in curve *f* appear only as a small remnant moving at c_s .

We have identified the pulses generated by the larger-amplitude applied pulses as pseudowaves, as described by Alexeff, Jones, and Lonngren¹⁷ and Lonngren *et al.*,¹⁸ mainly because we find that the leading edge velocity is given to within 3% by $(2e\Phi/m_i)^{1/2}$, where m_i is the mass of the argon ion, and Φ is the applied voltage difference. In addition, measurements with the electrostatic energy analyzer show particle bursts with kinetic energy $e\Phi$ for applied voltage Φ . These bursts are not associated with the solitons.

Pseudowaves can be eliminated by the application of pulses with amplitudes *less* than the electron temperature. Multiple soliton production can be achieved by widening rather than deepening the square well whose Schrödinger-equation bound states determine the number and amplitude of the emerging solitons. The formation of several solitons from a square compressive pulse is shown in Fig. 2. For narrow enough square pulses, a single soliton followed by a dispersive wave train moving slower than c_s is seen (Fig. 2, curve *a*). As the *width* of the compressive pulse is increased, the *amplitude* and velocity of the soliton increase. A second soliton is seen to begin to emerge in curve *b*. As the width is increased further, the first soliton amplitude remains approximately constant, but the amplitude of the second soliton increases and a third soliton is seen (Fig. 2, curve *d*). Further increasing the width increases the amplitude of the third soliton and a fourth soliton begins to emerge (Fig. 2, curve *e*).

The appearance of the solitons can be understood in terms of the Schrödinger equation with the attractive square-well potential. Since there always is at least one bound state for any one-dimensional well, we expect at least one soliton.

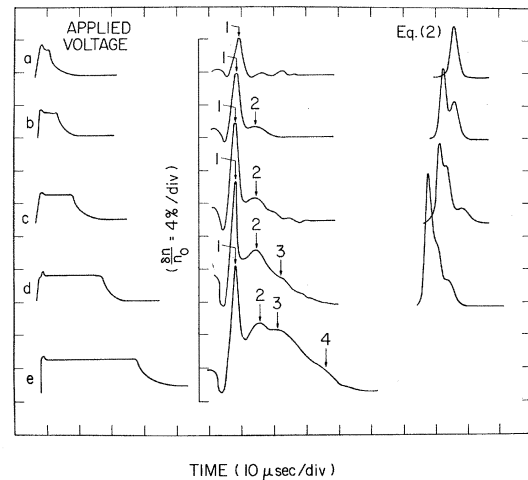


FIG. 2. Applied voltage pulses and electron density versus time, 10 cm from the screen. Electron density signals are not found to be sensitive to the sharpness of the edges of the applied pulses. Curves shown at the right are calculated from Eq. (2) with $\delta n_0/n_0 = 0.12$ and $\omega_{pi} = 5.5 \times 10^6$. An overall reduction of $\frac{1}{2}$ has been introduced to account for observed damping of the *largest*-amplitude soliton. Amplitude-dependent damping, which has not been included, reduces the amplitude, and broadens and separates in time smaller solitons relative to the larger ones. No curve has been given for curve *e* because it is seen in curve *d* that asymptotic behavior (i.e., separation of solitons) cannot be a reasonable assumption in curve *e*.

The maximum amplitude of the soliton is, from Eq. (2), $\delta n_{\max}/n_0 = 2(|E_1|/V_0) \delta n_0/n_0$. The bound-state energy increases as the width of the well increases, and when $|E_1| = 0.65V_0$, or $\delta n_{\max}/n_0 = 1.3 \delta n_0/n_0$, a second bound state appears at $|E_2| = 0$; i.e., a zero-amplitude soliton forms. In general, the j th soliton should appear when $a(\delta n_0/3n_0)^{1/2} = (j-1)\pi$, where a is the width of the original compressive pulse in Debye lengths. The relative amplitudes of solitons when new ones are just appearing are $g_j = 0.65; 0.86, 0.46; 0.92, 0.72, 0.36$; etc.

Predictions of the Schrödinger equation for the amplitudes cannot be directly tested because of the presence of non-negligible damping. The observed damping is consistent with ion Landau damping. (Large-amplitude solitons, traveling with higher velocities, encounter fewer resonant ions and hence damp less than small-amplitude solitons.) Nevertheless, we find that solitons appear to retain their identity while damping—i.e., reductions in amplitude are accompanied by reductions in velocity and increases in width. The

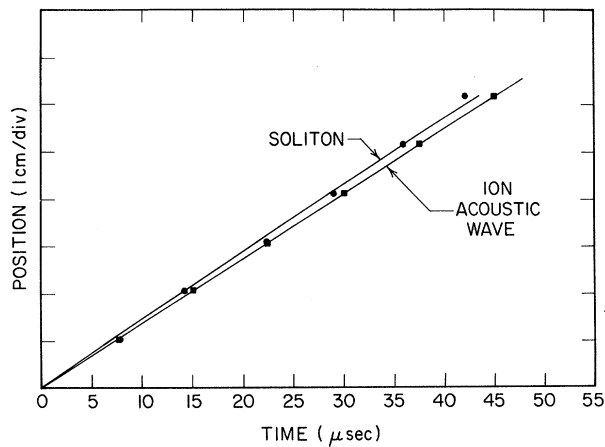


FIG. 3. Trajectories of a single soliton and ion acoustic wave are shown. We find that the soliton velocity is $(0.38 \pm 0.10) \delta n_{\max}/n_0$ from these data.

trajectory of a single soliton is compared with that of a very small-amplitude ion acoustic wave in Fig. 3. The curve for the soliton is a best least-squares fit made on the assumption that the soliton velocity is $b \delta n_{\max}/n_0$, with b constant. We find $b = 0.38 \pm 0.05$, in agreement with the predicted behavior for soliton solutions to Eq. (1).

Even though the amplitudes of observed solitons are no longer given by the theoretical expression after the damping begins, and the relative amplitudes depend on the (amplitude-dependent) damping, the number of solitons is determined by the original well. If we approximately determine the depth of the original well (i.e., the $\delta n_0/n_0$) from the width of the applied pulse at the appearance of the second soliton, we may note that additional increments in this width should produce successive solitons according to $a(\delta n_0/3n_0)^{1/2} = (j-1)\pi$. The results shown in Fig. 2, curve *a*, with temporal pulse width τ correspond to $a \cong c_s \tau / \lambda_D = 16 = \pi(3)^{1/2}(\delta n_0/n_0)^{-1/2}$, or $\delta n_0/n_0 \approx 0.12$. In Fig. 2, curve *d*, since the width of the square pulse is approximately 4 times that of Fig. 2, curve *a*, we expect that the fifth soliton will just be emerging with zero amplitude. The data show that at least three solitons have sufficient amplitude to be seen. In the right-hand panel of Fig. 2 we plot the right-hand side of Eq. (2) for comparison, assuming a value of $\delta n_0/n_0 = 0.12$, and neglecting damping. Though it is to be appreciated that Eq. (2) represents an asymptotic solution for spatial-

ly well-separated solitons, it can be seen that considerable similarity with the observed signal can exist (Fig. 2, curves *a-d*), even though the solitons still overlap.

We are indebted to Dr. R. A. Stern and Dr. J. F. Decker for generously providing us with a detailed description of their DP device, and to Professor I. Alexeff for good advice.

* Work supported in part by the National Aeronautics and Space Administration under Grant No. NGL 16-001-043.

¹H. Washimi and T. Taniuti, Phys. Rev. Lett. **17**, 996 (1966).

²D. J. Korteweg and G. de Vries, Phil. Mag. **39**, 422 (1895). [See also C. S. Gardner and G. Morikawa, Courant Institute Report No. NYO 9082, 1960 (unpublished).]

³R. C. Davidson, *Methods in Nonlinear Plasma Theory* (Academic, New York, 1972), Chap. 2.

⁴N. J. Zabusky and M. D. Kruskal, Phys. Rev. Lett. **15**, 240 (1965).

⁵N. J. Zabusky, Phys. Rev. **168**, 124 (1968).

⁶C. S. Gardner, J. M. Greene, M. D. Kruskal, and R. M. Miura, Phys. Rev. Lett. **19**, 1095 (1967).

⁷V. I. Karpman, Phys. Lett. **25A**, 708 (1967).

⁸Yu. A. Beresin and V. I. Karpman, Zh. Eksp. Teor. Fiz. **46**, 1880 (1964), and **51**, 1557 (1966) [Sov. Phys. JETP **19**, 1265 (1964), and **24**, 1049 (1967)].

⁹R. Miura, J. Math. Phys. **9**, 1202 (1968); R. Miura, C. S. Gardner, and M. D. Kruskal, J. Math. Phys. **9**, 1204 (1968); C. H. Su and C. S. Gardner, J. Math. Phys. **10**, 536 (1969); C. S. Gardner, J. Math. Phys. **12**, 1548 (1971); M. D. Kruskal, R. M. Miura, C. S. Gardner, and N. J. Zabusky, J. Math. Phys. **11**, 952 (1970).

¹⁰F. D. Tappert and N. J. Zabusky, Phys. Rev. Lett. **27**, 1774 (1971).

¹¹The results are announced in Ref. 6. To our knowledge, the full details have not been published. We have repeated the calculation outlined in Ref. 6.

¹²R. J. Taylor, D. R. Baker, and H. Ikezi, Phys. Rev. Lett. **24**, 206 (1970).

¹³H. Ikezi, R. J. Taylor, and D. R. Baker, Phys. Rev. Lett. **25**, 11 (1970).

¹⁴R. A. Stern and J. F. Decker, Phys. Rev. Lett. **27**, 1266 (1971).

¹⁵A. Y. Wong and R. W. Means, Phys. Rev. Lett. **27**, 973 (1971). [See also R. J. Taylor and F. V. Coroniti, Phys. Rev. Lett. **29**, 34 (1972).]

¹⁶H. Ikezi and R. J. Taylor, J. Appl. Phys. **41**, 738 (1970).

¹⁷I. Alexeff, W. D. Jones, and K. E. Lonngren, Phys. Rev. Lett. **21**, 878 (1968).

¹⁸K. Lonngren, D. Montgomery, I. Alexeff, and W. D. Jones, Phys. Lett. **25A**, 629 (1967).